

Atomic layer structure of manganese atoms on wurtzite gallium nitride (000 $\bar{1}$)

Abhijit Chinchore, Kangkang Wang, Wenzhi Lin, Jeongihm Pak, and Arthur R. Smith^{a)}

Department of Physics and Astronomy, Nanoscale and Quantum Phenomena Institute, Ohio University, Athens, Ohio 45701, USA

(Received 26 July 2008; accepted 6 October 2008; published online 5 November 2008)

Submonolayer quantities of Mn are deposited on wurtzite GaN (000 $\bar{1}$). The surface is monitored using reflection high energy electron diffraction, which shows a pattern consisting of $3 \times$ reconstruction along $[10\bar{1}0]$, but only $1 \times$ along $[11\bar{2}0]$. Diffraction analysis shows that the $3 \times$ streak intensity is maximized at ≈ 0.86 monolayer of Mn deposition. The results indicate that Mn forms linear chains along the $[10\bar{1}0]$ direction with a spacing of $\sqrt{3}a/2$ along chains and $3a/2$ between chains. Correcting the peak coverage for sticking coefficient and accounting for the observed periodicities, a $\sqrt{3} \times \sqrt{3}$ -R30° model, consisting of $2/3$ monolayer of Mn atoms, is proposed. © 2008 American Institute of Physics. [DOI: 10.1063/1.3006434]

Mn-doped gallium nitride (GaN) was proposed as a possible dilute magnetic semiconductor with Curie temperature above room temperature.¹ Consequently, many groups reported growth of Mn-doped GaN by molecular beam epitaxy (MBE) but with varying results.^{2–10} One problem was incorporation of Mn atoms at the bulk substitutional sites, apparently due to limited Mn solubility.

Recently, this low solubility has been exploited to develop an ideal magnetic/semiconductor bilayer.¹¹ Magnetic MnGa was found to grow with an abrupt interface and well-defined epitaxial orientation on top of wurtzite (*w*)-GaN. Reflection high energy electron diffraction (RHEED) patterns suggested a well-ordered structure at the initial stage of growth. Certainly, a thin well-ordered layer of Mn atoms on GaN could be of great interest for fundamental investigations and also for single monolayer magnetic devices.

In this letter, we present a study of exactly such a well-ordered layer of Mn atoms on *w*-GaN. It is shown that this well-ordered layer is produced by evaporation of Mn atoms onto the GaN(000 $\bar{1}$) 1×1 surface. RHEED is used to evaluate the surface structure as a function of coverage, and a reciprocal space model is derived corresponding to a real space model suggestive of Mn atom chains on the GaN surface.

The sample was prepared by cleaning a sapphire(0001) substrate using acetone and isopropanol followed by introducing it into an ultrahigh vacuum MBE chamber. The chamber is equipped with Ga and Mn effusion cells and a rf N-plasma source. The substrate was annealed at 900 °C under nitrogen plasma (power of 500 W) and with a N₂ flow rate of 1.1 SCCM to get a smooth nitrided substrate surface. A low temperature *w*-GaN buffer layer was then grown at 500 °C. After this, the main layer of GaN with a thickness of 2000 Å was grown at 650 °C.

The surface was monitored *in situ* using RHEED while the background pressure of the chamber was maintained at 9×10^{-6} Torr. Shown in Figs. 1(a) and 1(b) are RHEED patterns of the surface along $[10\bar{1}0]$ and $[11\bar{2}0]$ at the end of GaN growth and after being cooled to room temperature.

Outermost streaks in both Figs. 1(a) and 1(b) correspond to first-order streaks. Note that along $[10\bar{1}0]$ the spacing between first-order streaks is $\sqrt{3} \times$ that along $[11\bar{2}0]$.

Clearly evident in Figs. 1(a) and 1(b) are $3 \times$ and higher-order streaks indicating gallium adatom reconstructions, well investigated previously.^{12,13}

The sample was subsequently annealed at 700 °C to evaporate excess Ga adatoms. The result is shown in Figs. 1(c) and 1(d) in which the fractional-order streaks have been almost completely removed. Therefore, the surface has predominantly 1×1 structure, such as shown in Fig. 2(a). It consists of a layer of Ga atoms directly atop the N atoms of the last GaN bilayer.¹² This surface forms the starting point for Mn deposition.

The Mn atomic layer was prepared by depositing Mn in increments of 0.15 monolayer (ML) at 150 °C; we shall show that this results in a surface similar to that seen in Fig. 2(b). As seen clearly in Fig. 1(e), the $\frac{1}{3}$ -order streaks along $[10\bar{1}0]$ brighten markedly after just 0.3 ML of Mn, and the $\frac{2}{3}$ -order streaks also begin to appear. In contrast, along $[11\bar{2}0]$ there is no evidence of fractional streaks at 0.3 ML coverage, as shown in Fig. 1(f).

Further 0.15 ML increments lead to increasing intensity of both the $\frac{1}{3}$ - and $\frac{2}{3}$ -order streaks along $[10\bar{1}0]$, as shown in Fig. 1(g) for 0.8 ML of Mn. Also in Fig. 1(g) the $\frac{2}{3}$ -order streak intensity now exceeds that of the $\frac{1}{3}$ -order streak and that the first-order streaks have become weaker [c.f. to Fig.

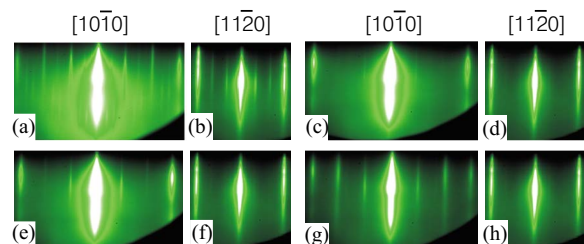


FIG. 1. (Color online) RHEED patterns for *w*-GaN(000 $\bar{1}$) surface: [(a) and (b)] just after GaN growth at 650 °C, [(c) and (d)] after annealing for ~ 2 h at 650 °C, [(e) and (f)] after depositing 0.3 ML Mn at 150 °C, and [(g) and (h)] after depositing 0.8 ML Mn at 150 °C.

^{a)}Electronic mail: smitha2@ohio.edu.

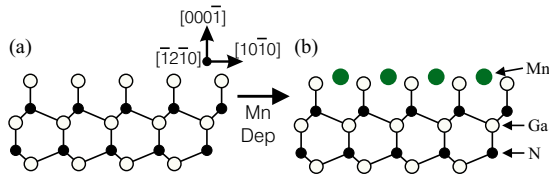


FIG. 2. (Color online) (a) Side-view model of GaN(0001) showing Ga adlayer (Ref. 12); (b) side-view model after adding 2/3 ML Mn.

1(e)]. Yet, as seen in Fig. 1(h), there is still no evidence of fractional streaks along $[11\bar{2}0]$.

To get more detailed information about the Mn atomic layer, the RHEED profile was measured as a function of time during Mn deposition, as shown in Fig. 3. This RHEED streak (time on vertical axis) movie image was acquired for 300 s. At $t=0$, the shutter was opened, and after depositing 1.95 ML Mn, the shutter was closed.

Shown in Fig. 4(a) are the $[10\bar{1}0]$ RHEED streak profiles taken from the movie at 0.15 ML Mn increments. At 0 ML Mn, the fractional order streak intensities are zero. After 0.15 ML of Mn is deposited, small bumps appear at the $\frac{1}{3}$ - and $\frac{2}{3}$ -order positions. The intensities of both peaks grow with each additional 0.15 ML Mn increment, with the peak intensities occurring for the 0.9 ML profile.

At the same time that the $\frac{1}{3}$ - and $\frac{2}{3}$ -order streaks are increasing in intensity, from Fig. 4(a) the first-order streaks are decreasing in intensity, finally becoming less intense than the $\frac{2}{3}$ -order streak.

The coverage-dependent intensities of the streaks are plotted directly in Fig. 4(b). As can be seen, the $\frac{1}{3}$ - and $\frac{2}{3}$ -order streak intensities start out at zero. At $t=0^+$, the $\frac{1}{3}$ - and $\frac{2}{3}$ -order streak intensities begin to rise at about the same rate. (Note: the small intensity jump when the shutter opens is followed by a corresponding drop when it closes and is unrelated to the surface structure; it is also seen for the background between streaks).

After ~ 0.1 ML, these two intensities begin to diverge with the $\frac{2}{3}$ -order streak intensity rising faster than that of the $\frac{1}{3}$ -order streak. Meanwhile, the $1\times$ streak intensity begins to reduce.

At ~ 0.86 ML Mn coverage, the $\frac{1}{3}$ - and $\frac{2}{3}$ -order streak intensities reach their peak, at which point the $\frac{2}{3}:\frac{1}{3}$ -order

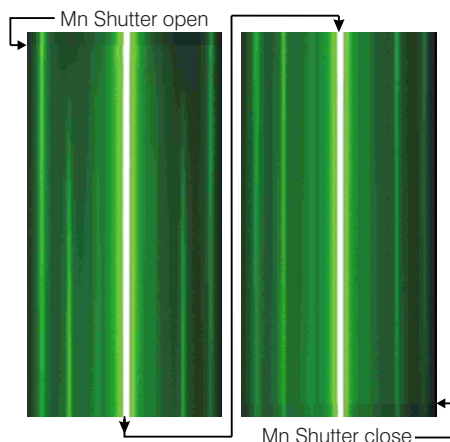


FIG. 3. (Color online) Scan mode RHEED movie image of Mn deposition on w-GaN(0001). Shown is the $[10\bar{1}0]$ azimuth. Total acquisition time is 300 s; total deposition amount is 1.95 ML Mn; sample temperature is 150 °C.

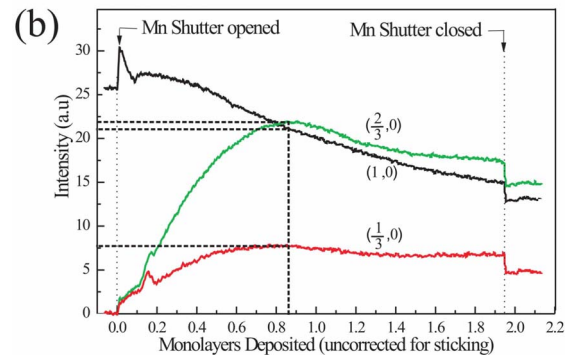
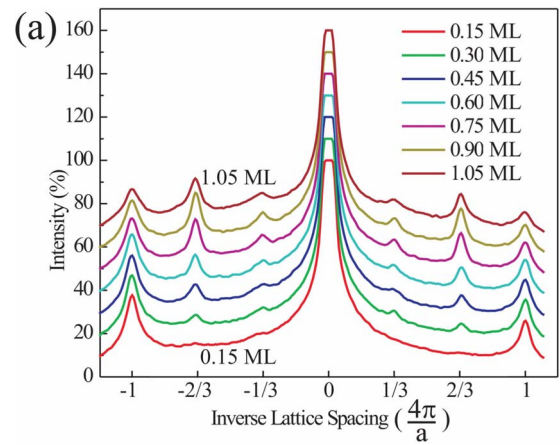


FIG. 4. (Color online) (a) RHEED profiles along $[10\bar{1}0]$ taken at 0.15 ML Mn-deposition increments (with y-offset added to separate the lines). (b) Continuous evolution of coverage-dependent streak intensities.

streak intensity (height) ratio is $\sim 2.9:1$. The $1\times$ streak intensity at this point is less than that of the $\frac{2}{3}$ -order streak.

The Mn reconstruction is clearly optimized at peak intensity. The actual coverage will be less than 0.86 ML, since the sticking coefficient is less than one. However, it is difficult to measure the sticking coefficient directly.

The clue however is the ratio of $\frac{2}{3}$ - to $\frac{1}{3}$ -order streak intensities. If these streaks had the same peak intensity, then a simple $\sqrt{3}\times\sqrt{3}$ -R30° model with a coverage of one Mn atom per $\sqrt{3}\times\sqrt{3}$ -R30° unit cell (corresponding to 1/3 ML) would accurately describe the Mn reconstruction.

However, in order to explain the ratio of fractional streak intensity (at peak intensity), we consider a variation in the 1/3 ML $\sqrt{3}\times\sqrt{3}$ -R30° model by including a second Mn atom per unit cell. This is the model shown in Fig. 5(a), corresponding to chains of Mn atoms running along the $[10\bar{1}0]$ with a spacing of $\sqrt{3}a/2$ along the chain and $3a/2$ between adjacent chains.

This $\sqrt{3}\times\sqrt{3}$ -R30° model has a Mn coverage of 2/3 ML. Comparing this number to the coverage dependent data presented in Figs. 3 and 4, we deduce a sticking coefficient of Mn on GaN at $T=150$ °C of $S=0.78$.

To see if the model shown in Fig. 5(a) correctly predicts the observed RHEED patterns we calculate the reciprocal space pattern of the model, taking into account the structure factors due to the two Mn atoms per unit cell. This pattern is depicted in Fig. 5(b).

Based on the $2/3\text{ML}\sqrt{3}\times\sqrt{3}$ -R30° model, we calculate a reciprocal space map in which the Mn atom-derived spots have two kinds of intensities, one equal to $I^+ = |f_1 + f_2|^2$, the other $I^- = |f_1 - f_2|^2$, where the f 's are the form factors. Since

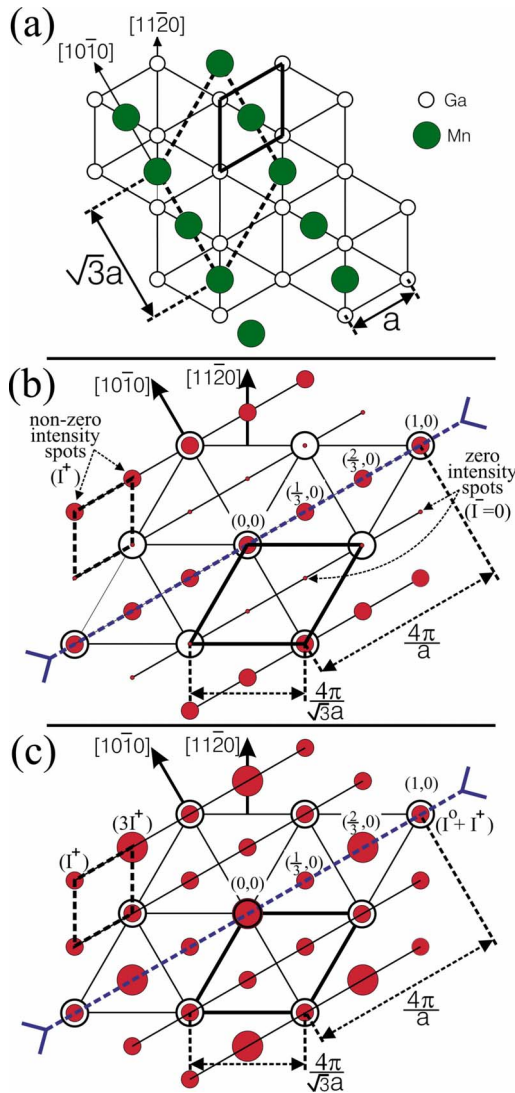


FIG. 5. (Color online) (a) Real space model consisting of 2/3 ML Mn on w -GaN(000 $\bar{1}$) in $\sqrt{3} \times \sqrt{3}$ -R30° arrangement; (b) derived reciprocal space pattern, taking into account the structure factors; intensities of reciprocal space points are shown as dots of different sizes; reciprocal space points of the underlying GaN lattice are shown as open circles; and points for the Mn overlayer are shown as solid dots; (c) superposition of reciprocal space patterns from three equivalent 2/3 ML $\sqrt{3} \times \sqrt{3}$ -R30° (120°-rotated) domains.

the two Mn atoms per unit cell have identical local environment, we conclude that f_1 must equal f_2 , and therefore $I^- = 0$. The reciprocal pattern then consists of rows of spots in which the intensities alternate between I^+ and 0 along $[10\bar{1}0]$ (the second atom per unit cell causes one-half the spots to have zero intensity).

What is clear from the map of Fig. 5(b) is that the $(\frac{1}{3}, 0)$ and $(\frac{2}{3}, 0)$ spots (which really correspond to rods in three-dimensional reciprocal space) have the same intensity, which does not agree with the data presented in Fig. 4(b).

However, since the real-space model of Fig. 5(a) actually has only twofold rotational symmetry and this being adhered to a threefold symmetric wurtzite lattice surface, we expect there to exist three equivalent domains. Therefore, the actual RHEED pattern observed is expected to correspond to the superposition of three 120°-rotated spot patterns.

As can be seen from Fig. 5(c), such superposition of the three twofold symmetric patterns has itself a threefold symmetry, and in addition, we find that the $(\frac{1}{3}, 0)$ and $(\frac{2}{3}, 0)$ spots

no longer have the same intensity. In fact, the $(\frac{1}{3}, 0)$ spot has intensity $I_{\text{tot}} = I^+$, while the $(\frac{2}{3}, 0)$ spot has intensity $I_{\text{tot}} = 3I^+$. This is in excellent agreement with the intensity results shown in Fig. 4 in which we see a 2.9:1 intensity (height) ratio. Moreover, if we reanalyze by taking areas under the peaks, we get a ratio of $\sim 2.92:1$.

We also see that the (1,0) spot should have intensity $I_{\text{tot}} = I_o + I^+$, where I_o = intensity from the underlying w -GaN lattice, and from the data of Fig. 4(b) this streak has intensity close to that of the $(\frac{2}{3}, 0)$ streak.

Other 2/3 ML models have been considered, including models in which one or both Mn atoms sit in threefold hollow site(s); however, the observed $\sim 3:1$ intensity ratio was not predicted.

Although the model shown in Fig. 5(a) appears to be a bridge site model, we also point out that in the case of Ga adatoms on the surface shown in Fig. 2(a), those adatoms are found to sink into the surface allowing the Ga adlayer atoms to relax laterally, thereby lowering surface energy; this model was referred to as an in-plane adatom model.¹² We postulate that in this case of Mn adatoms, a similar effect may occur in which Mn atoms sink into the surface, leading to a stable in-plane type structure, as suggested in Fig. 2(b). Theoretical calculations would be helpful.

Finally, we note that the model of Fig. 5(a) is consistent with the orientation relationship derived for ferromagnetic δ -MnGa layers grown by MBE on w -GaN.¹¹

To summarize, deposition of Mn onto w -GaN(000 $\bar{1}$) forms an ordered Mn atomic layer with coverage of 2/3 ML. The RHEED data suggests a model consisting of Mn chains running along $[10\bar{1}0]$. Twofold symmetry of this model results in three different domains on the GaN surface.

The authors would like to thank the U.S. Department of Energy (Grant #DE-FG02-06ER46317) and the National Science Foundation (Grant #0730257) for support of this work.

¹T. Dietl, H. Ohno, F. Matsukura, J. Cibert, and D. Ferrand, *Science* **287**, 1019 (2000).

²S. Sonoda, S. Shimizu, T. Sasaki, Y. Yamamoto, and H. Hori, *J. Cryst. Growth* **237**, 1358 (2002).

³H. Hori, S. Sonoda, T. Sasaki, Y. Yamamoto, S. Shimizu, K. Suga, and K. Kindo, *Physica B (Amsterdam)* **324**, 142 (2002).

⁴M. L. Reed, N. A. El-Masry, H. H. Stadelmaier, M. K. Ritums, M. J. Reed, C. A. Parker, J. C. Roberts, and S. M. Bedair, *Appl. Phys. Lett.* **79**, 3473 (2001).

⁵N. Theodoropoulou, K. P. Lee, M. E. Overberg, S. N. G. Chu, A. F. Hebard, C. R. Abernathy, S. J. Pearton, and R. G. Wilson, *J. Nanosci. Nanotechnol.* **1**, 101 (2001).

⁶G. T. Thaler, M. E. Overberg, B. Gilla, R. Frazier, C. R. Abernathy, S. J. Pearton, J. S. Lee, S. Y. Lee, Y. d. Park, Z. G. Khim, J. Kim, and F. Ren, *Appl. Phys. Lett.* **80**, 3964 (2002).

⁷M. E. Overberg, C. R. Abernathy, S. J. Pearton, N. A. Theodoropoulou, K. T. McCarthy, and A. F. Hebard, *Appl. Phys. Lett.* **79**, 1312 (2001).

⁸M. B. Haider, C. Constantin, H. Al-Brithen, H. Yang, E. Trifan, D. Ingram, A. R. Smith, C. V. Kelly, and Y. Ijiri, *J. Appl. Phys.* **93**, 5274 (2003).

⁹M. B. Haider, C. Constantin, H. Al-Brithen, G. Caruntu, C. J. O'Conner, and A. R. Smith, *Phys. Status Solidi A* **202**, 1135 (2005).

¹⁰K. Sato, W. Schweika, P. H. Dederichs, and H. Katayama-Yoshida, *Phys. Rev. B* **70**, 201202 (2004).

¹¹E. Lu, D. C. Ingram, A. R. Smith, J. W. Knepper, and F. Y. Yang, *Phys. Rev. Lett.* **97**, 146101 (2006).

¹²A. R. Smith, R. M. Feenstra, D. W. Greve, J. Neugebauer, and J. E. Northrup, *Phys. Rev. Lett.* **79**, 3934 (1997).

¹³A. R. Smith, R. M. Feenstra, D. W. Greve, M.-S. Shin, M. Skowronski, J. Neugebauer, and J. E. Northrup, *Appl. Phys. Lett.* **72**, 2114 (1998).